

Plant Raf-like kinase integrates abscisic acid and hyperosmotic stress signaling upstream of SNF1-related protein kinase2

Masashi Saruhashi^a, Totan Kumar Ghosh^a, Kenta Arai^a, Yumiko Ishizaki^a, Kazuya Hagiwara^a, Kenji Komatsu^b, Yuh Shiwa^c, Keiichi Izumikawa^d, Harunori Yoshikawa^{d,e}, Taishi Umezawa^{f,g}, Yoichi Sakata^h, and Daisuke Takezawa^{a,i,1}

^aGraduate School of Science and Engineering, Saitama University, Saitama 338-8570, Japan; ^bDepartment of Bioproduction Technology, Junior College of Tokyo University of Agriculture, Tokyo 156-8502, Japan; ^cGenome Research Center, NODAI Research Institute, Tokyo University of Agriculture, Tokyo 156-8502, Japan; ^dFaculty of Agriculture, Tokyo University of Agriculture and Technology, Tokyo 183-8538, Japan; ^eCentre for Gene Regulation and Expression, School of Life Sciences, University of Dundee, Dundee DD1 5EH, Scotland, United Kingdom; ^fGraduate School of Bio-Applications and Systems Engineering, Tokyo University of Agriculture and Technology, Tokyo 184-8588, Japan; ^gPrecursory Research for Embryonic Science and Technology (PRESTO), Japan Science and Technology Agency, Tokyo 102-0007 Japan; ^hDepartment of BioScience, Tokyo University of Agriculture, Tokyo 156-8502, Japan; and ⁱInstitute for Environmental Science and Technology, Saitama University, Saitama 338-8570, Japan

Edited by Julian I. Schroeder, University of California, San Diego, La Jolla, CA, and approved October 8, 2015 (received for review June 10, 2015)

Plant response to drought and hyperosmosis is mediated by the phytohormone abscisic acid (ABA), a sesquiterpene compound widely distributed in various embryophyte groups. Exogenous ABA as well as hyperosmosis activates the sucrose nonfermenting 1 (SNF1)-related protein kinase2 (SnRK2), which plays a central role in cellular responses against drought and dehydration, although the details of the activation mechanism are not understood. Analysis of a mutant of the moss *Physcomitrella patens* with reduced ABA sensitivity and reduced hyperosmosis tolerance revealed that a protein kinase designated “ARK” (for “ABA and abiotic stress-responsive Raf-like kinase”) plays an essential role in the activation of SnRK2. ARK encoded by a single gene in *P. patens* belongs to the family of group B3 Raf-like MAP kinase kinase kinases (B3-MAPKKKs) mediating ethylene, disease resistance, and salt and sugar responses in angiosperms. Our findings indicate that ARK, as a novel regulatory component integrating ABA and hyperosmosis signals, represents the ancestral B3-MAPKKKs, which multiplied, diversified, and came to have specific functions in angiosperms.

abscisic acid | *Physcomitrella patens* | Raf-like kinase | SnRK2

Plant responses to water deficit stress are among the most important adaptations required for life on land. Ever since the colonization of land by the algal ancestor in the Middle Ordovician, embryophytes have developed physiological mechanisms for sensing and transducing environmental signals to protect themselves from a forthcoming severe water deficit. Abscisic acid (ABA), which is found in various embryophyte groups, is one of key molecules that play a role in water stress responses in the terrestrial environment. In angiosperms, ABA induces closure of stomata in leaves for prevention of water loss, and it maintains dormancy and desiccation tolerance in maturing seeds. In the moss *Physcomitrella patens* ABA induces tolerance to freezing, hyperosmosis, desiccation of protonema cells, and the accumulation of a number of stress-related transcripts such as those encoding late embryogenesis abundant (LEA)-like hydrophilic proteins, which are thought to be important for protecting cells from dehydration-induced damage to membranes and other cellular macromolecules (1–3). These facts suggest conserved roles of ABA in dehydration stress tolerance, although whether common signaling mechanisms operate in various land plant groups has not been clarified.

Studies of the signal-transduction process in angiosperms have shed light on a critical role of sucrose nonfermenting 1-related protein kinase2 (SnRK2) in the ABA and dehydration responses. SnRK2 was first identified as an ABA-activated protein kinase in fava beans that mediates ABA-induced closure of leaf stomata (4) and also was identified as a factor encoded by *OPEN STOMATA1* (*OST1*)

in *Arabidopsis thaliana*, mutation of which causes an ABA-hypersensitive stomata closure response (5). Further analysis revealed that SnRK2 plays a pivotal role in the signaling of ABA by phosphorylating key transcription factors and ion channels (6, 7). SnRK2s also are activated by hyperosmotic stress, indicating a role in drought tolerance associated with the induction of stress-responsive genes (8, 9). SnRK2s of angiosperms are categorized into three subclasses: I, II, and III (8, 10). In-gel kinase assays using histone H2S as a substrate revealed that subclass I SnRK2s are activated by osmotic stress but not by ABA, whereas the subclass II and subclass III SnRK2s are activated by both ABA and osmotic stress, with subclass III being activated more strongly than subclass II by ABA. Analysis of an *Arabidopsis* mutant null for three subclass III SnRK2 isoforms (*srk2dsrk2esrk2i* or *snrk2.2snrk2.3snrk2.6*) has shown that subclass III members play an essential role in the signal transduction of the ABA response (11, 12). Phosphopeptide mapping of subclass III SnRK2 revealed that ABA induced phosphorylation of Ser and Thr residues in the activation loop between kinase domains VII and VIII (12, 13). Furthermore, discovery of soluble ABA receptors (PYR/PYL/RCAR) has led to the establishment of the core model for the activation of SnRK2. In this model, activity of subclass III

Significance

Plants can sense loss of water caused by drought and stimulate internal mechanisms for protecting cells from damage with the aid of the stress hormone abscisic acid (ABA). Analysis of a mutant of the basal land plant, the moss *Physcomitrella patens*, revealed that an impairment of a protooncogene Raf-like protein kinase, designated “ARK” (for “ABA and abiotic stress-responsive Raf-like kinase”), causes a loss of both ABA sensitivity and osmotic stress tolerance. We show evidence that ARK has a role in integrating ABA and osmotic signals upstream of the sucrose nonfermenting 1-related protein kinase2, known to be a central regulator of stress signaling in plants.

Author contributions: Y. Sakata and D.T. designed research; M.S., T.K.G., K.A., Y.I., K.H., K.K., Y. Shiwa, K.I., H.Y., T.U., Y. Sakata, and D.T. performed research; M.S., T.K.G., Y.I., K.K., Y. Shiwa, K.I., H.Y., T.U., Y. Sakata, and D.T. analyzed data; and M.S. and D.T. wrote the paper.

The authors declare no conflict of interest.

This article is a PNAS Direct Submission.

Freely available online through the PNAS open access option.

Data deposition: The sequence reported in this paper has been deposited in the GenBank database (accession no. [KT581394](#)), and the microarray data have been deposited in the Gene Expression Omnibus database (accession no. [GSE68914](#)).

¹To whom correspondence should be addressed. Email: takezawa@mail.saitama-u.ac.jp.

This article contains supporting information online at www.pnas.org/lookup/suppl/doi:10.1073/pnas.1511238112/-DCSupplemental.

SnRK2s is suppressed by group A protein phosphatase 2C (PP2Cs) in the absence of ABA, and binding of ABA to the PYR/PYL/RCAR inhibits PP2Cs, thus allowing activation of SnRK2 (14–16). Phosphorylation in the activation loop of SnRK2 is thought to be completed by autophosphorylation (11), although the details of the mechanism remain to be clarified.

Entire genome sequencing of *P. patens* (17) has revealed that four PYR/PYL/RCARs, two group A PP2Cs, and four SnRK2s are encoded in the moss genome, indicating that the core members needed for the ABA response are conserved from bryophytes to angiosperms (18). All SnRK2s encoded in the *P. patens* genome were assigned to the subclass III category, suggesting that this subclass represents the ancestral members of SnRK2. The *P. patens* *PpOST1-1* gene, encoding SnRK2, was shown to complement the ABA-insensitive stomatal response of *ost1* in transgenic *Arabidopsis*, and disruption of *PpOST1-1* in *P. patens* resulted in an ABA-insensitive stomatal response in the sporophyte (19). That study suggested possible conservation of SnRK2 function in land plants. A recent study also indicated a role of group A PP2Cs as negative regulators of ABA signaling in bryophytes. A transgenic line lacking both group A PP2C genes (*PpABI1A* and *PpABI1B*) exhibited constitutive desiccation tolerance with the accumulation of a number of stress-associated transcripts regardless of ABA treatment (20). In this knockout line, however, SnRK2 was activated by exogenous ABA in a manner similar to that in the WT line (20), indicating group A PP2Cs have a minor role in the regulation of SnRK2 and the presence of a previously unidentified mechanism for its activation.

To understand better the molecular mechanisms underlying the ABA response in bryophytes, we mutagenized protonema cells of *P. patens* by UV irradiation and obtained mutant lines that could grow better than the WT line on medium containing ABA. One of the mutants, designated “AR7,” showed an ABA-insensitive growth response and reduced freezing-stress tolerance (21). AR7 also showed reduced responses to dehydration and cold (22), indicating that the molecule integrating ABA and stress-signaling processes is impaired in AR7. This report characterizes AR7 further and identifies the gene altered in AR7. Comparative

genomic sequence analysis between AR7 and the WT line revealed that AR7 has a mutation in the gene encoding a group B3 Raf-like MAP kinase kinase kinase (B3-MAPKKK), subsequently designated “ARK” (for “ABA and abiotic stress responsive Raf-like kinase”). Further analyses indicated that ARK plays a key role in SnRK2-mediated ABA and hyperosmosis responses in the moss. On the basis of these collective findings, we propose that, in addition to PYR/PYL/RCAR and PP2C, ARK is an essential element of signaling components for the regulation of SnRK2 in basal land plants.

Results

Analysis of Transcriptome and Protein Kinase Activity in AR7. The AR7 line has been characterized as a mutant with reduced ABA sensitivity in various aspects such as growth inhibition, morphological changes leading to brood cell formation, accumulation of soluble sugars and LEA-like boiling-soluble proteins, and tolerance of freezing and dehydration stress (21, 22). Microarray analysis of transcript profiles revealed that the expression of a large portion of the ABA-responsive genes was affected in AR7. Expression of 518 of 579 ABA up-regulated genes in the WT line was reduced significantly in AR7 (Fig. 1A, Left). These genes included 27 LEA-like genes encoding highly hydrophilic polypeptides, which are considered to be associated with dehydration stress tolerance (Table S1). RNA gel-blot analysis of four representative LEA-like transcripts, *17B9* (*Pp1s294_52V6.1*), *6A5* (*Pp1s267_21V6.1*), *LEAIII* (*Pp1s118_232V6.1*), and *19C6* (*Pp1s52_261V6.1*), confirmed impaired ABA-induced gene expression in AR7 (Fig. 1B). Furthermore, levels of 150 of 165 ABA down-regulated transcripts were higher in AR7 than in the WT line (Fig. 1A, Right). These results indicated that the gene impaired in AR7 encodes an important positive regulator of ABA-responsive gene expression in *P. patens*.

In angiosperms, most of the physiological processes required for the ABA response, including gene expression for various stress-associated proteins, are controlled by subclass III SnRK2s (10). ABA-induced activation of the protein kinase corresponding to the expected size of SnRK2 (39 kDa) has been demonstrated recently in *P. patens* protonemata by in-gel kinase assays using histone IIIS as a substrate (20). We found that protonemata of

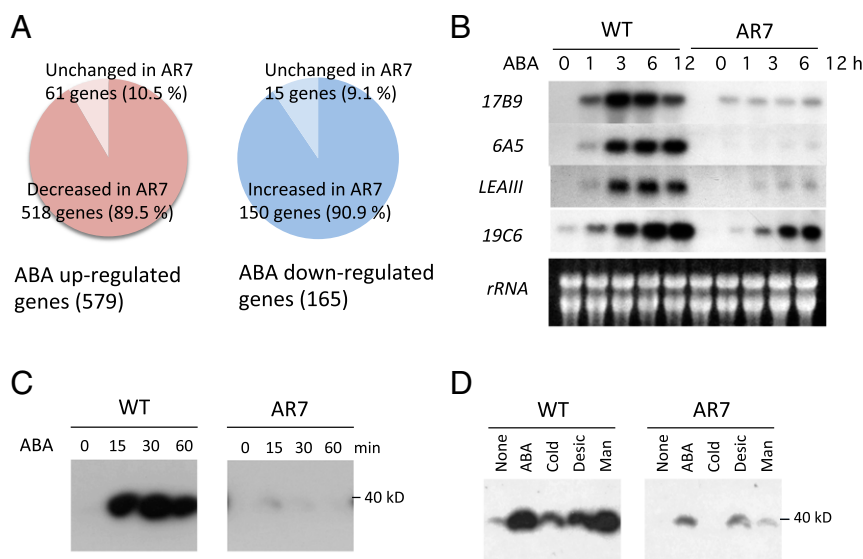


Fig. 1. ABA-induced gene expression and SnRK2 activity in the WT line and AR7. (A) Results of comparative microarray analysis showing ABA up-regulated and down-regulated transcripts. (B) RNA gel blot analysis of WT and AR7 protonemata. Total RNA isolated from protonemata treated with 10 μ M ABA for the indicated times was probed with radiolabeled cDNA fragments of the representative ABA-inducible transcripts, *17B9* (*Pp1s294_52V6.1*), *6A5* (*Pp1s267_21V6.1*), *LEAIII* (*Pp1s118_232V6.1*), and *19C6* (*Pp1s52_261V6.1*) (43). (C and D) In-gel kinase assays of WT and AR7 protonemata for detection of SnRK2 activity. *P. patens* protonemata were treated with 10 μ M ABA for the indicated times (C) or were subjected to various treatments (D). ABA, 10 μ M ABA for 30 min; Cold, 0 $^{\circ}$ C for 1 h; Desic, desiccation in a laminar flow for 30 min; Man, 0.5 M mannitol for 30 min.

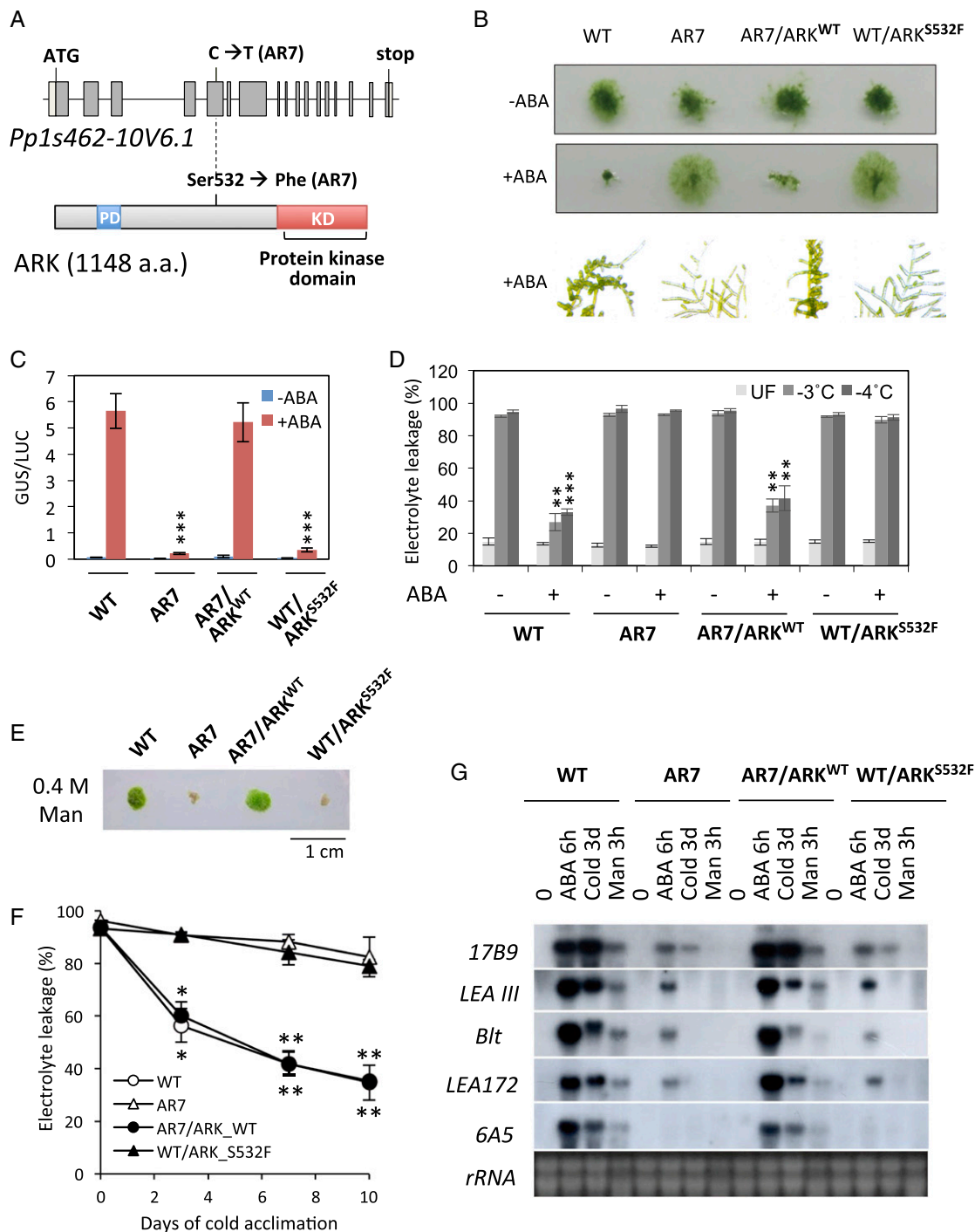


Fig. 2. Characterization of *Pp1s462-10V6.1* of *P. patens*. (A) Structures of the *Pp1s462-10V6.1* gene mutated in AR7 and the encoded protein ARK deduced from the sequence of the isolated cDNA (GenBank KT581394). The C-to-T transition in the fifth exon caused an amino acid change from Ser to Phe at position 532 N-terminal to the protein kinase domain (KD). PD indicates a putative PAS domain. (B) Growth of protonemata with or without ABA of WT, AR7, the AR7 knock-in line with the ARK sequence changed to that of WT (AR7/ARK^{WT}), and the WT knock-in line with the ARK sequence changed to that of AR7 type (WT/ARK^{S532F}). (C) Transient assays for detection of ABA-induced gene expression. The protonemata of the lines used in B were bombarded with the *Em-GUS* and *Ubi-LUC* constructs and incubated with or without 10 μ M ABA for 1 d, followed by the GUS and LUC assays. Levels of gene expression are represented by GUS/LUC ratio. Error bars indicate the SE ($n = 3$). *** $P < 0.01$ compared with ABA-treated WT (t -test). (D) ABA-induced freezing tolerance of the lines used in B. Protonemata were treated for 1 d with 10 μ M ABA and either were kept at 4 $^{\circ}$ C (UF) or were subjected to equilibrium freezing to -3° C or -4° C. Survival of the protonemata was estimated by measuring electrolyte leakage from the injured cells. Error bars indicate the SE ($n = 3$). *** $P < 0.001$ and ** $P < 0.01$ compared with the ABA-negative (–) tissue of the same line (t -test). (E) Osmotic stress tolerance of the protonemata. Pieces of protonemata were grown on BCDAT medium containing 0.4 M mannitol. (F) Cold-acclimation capacities of the protonemata. The cells were incubated on BCDAT medium at 0 $^{\circ}$ C for the indicated number of days and then were subjected to freezing at -3° C to determine electrolyte leakage. Error bars indicate the SE ($n = 3$). * $P < 0.05$ and ** $P < 0.01$ compared with the nonacclimated tissue of the same line (t -test). (G) Accumulation of stress-associated transcripts. RNA extracted from protonemata after treatment with ABA, cold, or hyperosmotic 0.5 M mannitol was electrophoresed, blotted onto a nylon membrane, and reacted with radiolabeled probes of the indicated transcripts. Ethidium bromide-stained rRNA is shown for verification of equal loading.

AR7 showed little activity of the ABA-induced kinase compared with WT protonemata (Fig. 1C). We further compared the kinase activity in the WT line and AR7 in response to other abiotic stresses and found that induction of the kinase activity by cold, desiccation, and hyperosmosis generated by 0.5 M mannitol treatment was also defective in AR7 (Fig. 1D). From these results, we speculated that the gene mutated in AR7 is involved in ABA-induced activation of SnRK2, which controls levels of the majority of transcripts during the response to exogenous ABA.

Identification of the Gene Mutated in AR7. To identify the mutation locus in the genome of AR7, comparative genomic sequence analysis of AR7 and the WT line was carried out using the Illumina HiSeq 2000 sequencer. More than 286 million and 101 million reads of 100-bp nucleotide fragments of the WT line and AR7, covering roughly 58 and 21 times the genome size, respectively, were analyzed against the reference genome sequence of *P. patens* subsp. *patens* V1.6. The analysis revealed a total of 2,068 mutations in the AR7 genome, causing 47 nonsynonymous substitutions of amino acids in the encoded proteins (Dataset S1). To examine whether mutations of any of these 47 candidate genes caused ABA-insensitive phenotypes in AR7, the cDNA clones for these genes were isolated from the WT line and transiently expressed in the AR7 protonemata by particle bombardment. The candidate cDNA was cotransformed with the ABA-induced *Em* promoter fused to the β -glucuronidase reporter gene (*Em-GUS*) (23, 24) to determine whether any of the clones restore ABA-induced GUS expression in AR7, which otherwise shows very little GUS expression. Introduction of one cDNA clone corresponding to the gene model *Pp1s462-10V6.1* was found to restore the ABA insensitivity of AR7. The *Pp1s462-10V6.1* gene consisted of 17 exons, and analysis of the longest cDNA revealed that it encodes a 1,148-amino acid protein having a C-terminal protein kinase domain similar to plant Raf-like MAPKKs belonging to B3-MAPKKs (Fig. 2A). The stretch of amino acids from positions 86–185 in the N-terminal nonkinase domain contained a putative PAS domain possibly involved in molecular interactions (25), which typically is conserved in group B2 MAPKKs (B2-MAPKKs) categorized in angiosperms (26). The *Pp1s462-10V6.1* gene was designated as “ARK.” Sequence analysis revealed that Ser-532 (TCC) located in a position N-terminal to the kinase domain was changed to Phe-532 (TTC) by a single C-to-T transition in the fifth exon of ARK in AR7 (Fig. 2A).

To determine why the Ser-to-Phe mutation at position 532 found in AR7 caused ABA insensitivity, we analyzed the accumulation of ARK proteins in the WT line and AR7 by immunoblot analysis using an antibody raised against the C-terminal amino acids of ARK. We detected immunoreactive bands of ~120 kDa consistent with the length of 1,148 amino acids of ARK. However, the accumulation of ARK proteins appeared to be similar in the WT line and AR7 and did not change significantly during ABA treatment (Fig. S1). To confirm that the Ser-to-Phe mutation at position 532 caused the ABA-insensitive phenotype, a gene knock-in experiment was conducted. A genomic fragment of ARK from the WT line was fused with the neomycin phosphotransferase gene cassette so the marker would be inserted into a position downstream of the polyadenylation site. The resultant construct was introduced into AR7 by polyethylene glycol-mediated protoplast transformation to obtain transgenic plants resistant to the antibiotic G418. After confirmation of gene targeting to the ARK locus (Fig. S2), the generated knock-in line (AR7/ARK^{WT}) was used for various physiological analyses of ABA responses. Exogenous ABA inhibited protonemal growth of AR7/ARK^{WT} and facilitated subsequent formation of brood cells similar to that in the WT line (Fig. 2B). Transient expression analysis showed ABA-induced *Em-GUS* expression in the AR7/ARK^{WT} protonemata similar to that in the WT line

(Fig. 2C). Furthermore, impaired ABA-induced freezing tolerance of AR7 was recovered in AR7/ARK^{WT} to a level similar to that in the WT line (Fig. 2D) concomitant with accumulation of LEA-like boiling-soluble proteins (Fig. S3).

Hyperosmotic- and cold-stress responses also were examined in the AR7/ARK^{WT} line. Although growth of AR7 protonemata was susceptible to 0.4 M mannitol contained in the medium, AR7/ARK^{WT} protonemata grew on the medium in a manner similar to that of the WT line (Fig. 2E). Furthermore, AR7 showed reduced cold acclimation capacity (i.e., cold-induced freezing tolerance) compared with that of the WT line (22), but AR7/ARK^{WT} acclimated to cold in a manner similar to that of the WT.

To confirm the phenotypic reversion by the change in a single amino acid of ARK, a similar gene knock-in experiment was carried out to introduce an AR7-type mutation (Ser-532 to Phe) into the ARK locus of the WT line. The resultant WT/ARK^{S532F} line was found to mimic AR7 phenotypes in protonemata growth. In addition, that line was insensitive to ABA, cold, and hyperosmotic treatment as observed in AR7 (Fig. 2A–F). When expression profiles of representative transcripts of WT, AR7, AR7/ARK^{WT}, and WT/ARK^{S532F} were compared in terms of responsiveness to ABA, hyperosmosis, and cold, the results were consistent with the growth and stress-tolerance phenotypes in these lines (Fig. 2G). These results indicated that ARK plays a crucial role in cellular responses to ABA and abiotic stresses in *P. patens* and that the single Ser-to-Phe change at the amino acid position 532 of ARK was sufficient to alter the responses.

ARK Kinase Activity Toward SnRK2. To examine changes in ABA-induced protein kinase activity in the ARK knock-in lines, in-gel kinase assays were carried out using histone H1 as a substrate. Protonemata of AR7/ARK^{WT} had ABA-induced kinase activity similar to that of the WT line, whereas protonemata of the WT/ARK^{S532F} line showed very little kinase activity, comparable to that of AR7 (Fig. 3A). From these results, we speculated that ARK is either directly or indirectly involved in the activation of SnRK2s. We found that PpSnRK2B (*Pp1s240_91V6.1*), one of the SnRK2s of *P. patens*, is activated by ABA, as shown by in-gel kinase assays of transgenic *P. patens* expressing PpSnRK2B fused to GFP (PpSnRK2B-GFP). PpSnRK2B also was activated by hyperosmosis (Fig. S4). Cellular localization of ARK-GFP and of PpSnRK2B-GFP was analyzed in *P. patens* protonema cells by confocal microscopy. ARK-GFP was localized mainly in the cytosol, and PpSnRK2B-GFP was localized in the cytosol and nucleus in the protonema cells, suggesting possible colocalization of PpSnRK2B with ARK in the cytosol (Fig. 3B). Similar experiments using the onion epidermal cells also indicated possible localization of PpSnRK2B and ARK in the cytosol (Fig. S5).

To determine the role of ARK in the possible regulation of PpSnRK2B, phosphorylation assays were carried out using recombinant proteins. The protein kinase domain of ARK fused to GST (GST-ARK^{KD}) and PpSnRK2B fused to maltose-binding protein (MBP-PpSnRK2B) were expressed in *Escherichia coli*, and affinity-purified recombinant proteins were used for in vitro phosphorylation assays. Results of assays indicated that MBP-PpSnRK2B showed some autophosphorylation activity, but GST-ARK^{KD} phosphorylated MBP-PpSnRK2B more strongly (Fig. 3C). To examine the effect of this phosphorylation of MBP-PpSnRK2B on its kinase activity, in-gel kinase assays of non-phosphorylated, autophosphorylated, and ARK-phosphorylated MBP-PpSnRK2B were carried out using histone H1 as a substrate. Results of assays indicated that the activity of MBP-PpSnRK2B was increased by phosphorylation catalyzed by GST-ARK^{KD} but was not affected by autophosphorylation (Fig. 3D). Phosphopeptide mapping revealed that GST-ARK^{KD} phosphorylated specific serine residues (Ser-165 and Ser-169) of the MBP-PpSnRK2B protein (Fig. 3E and Fig. S6). The phosphorylation site corresponding to Ser-169, which lies between subdomains VII

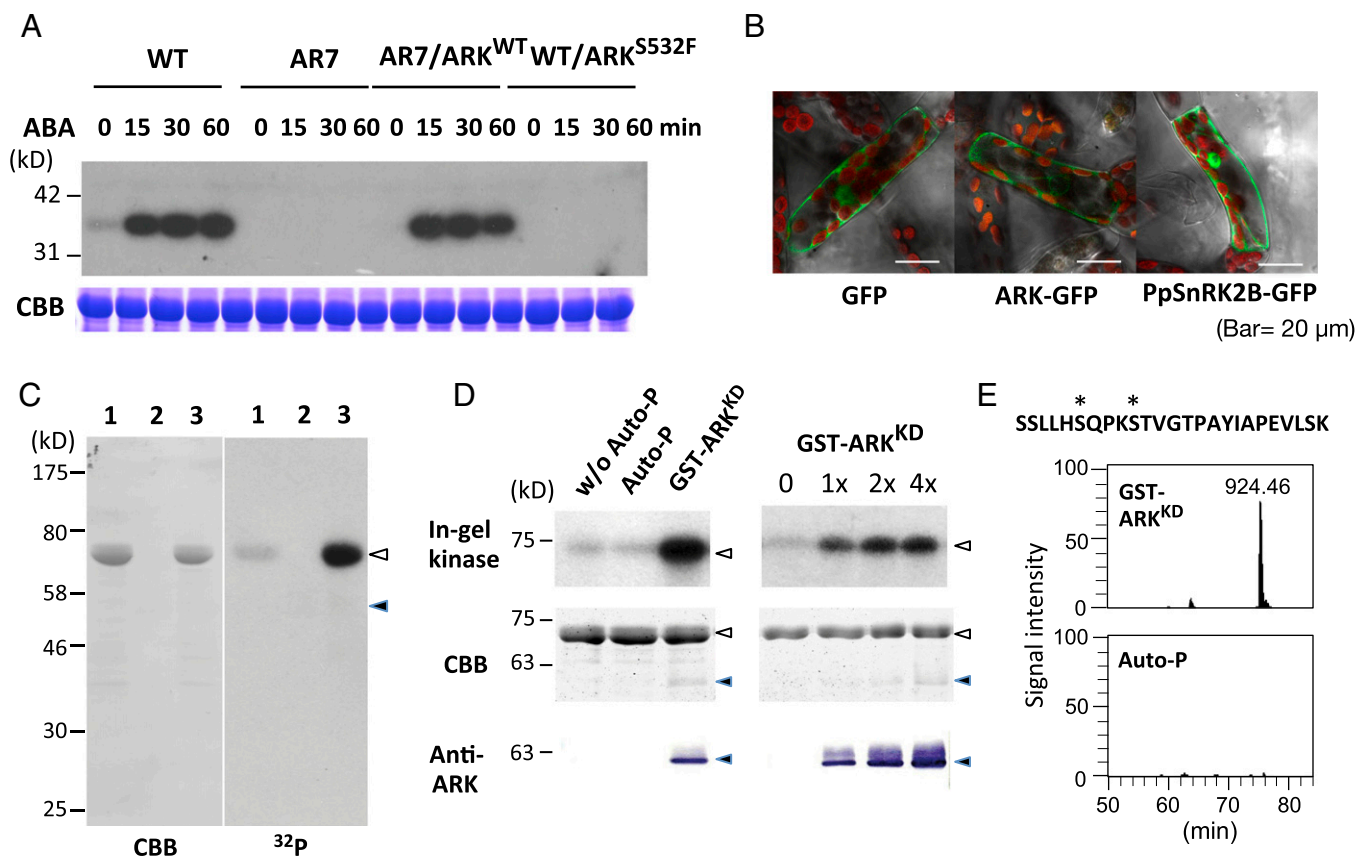


Fig. 3. ARK as a possible regulator of SnRK2. (A, Upper) In-gel kinase assays of protonemata of WT, AR7, and ARK knock-in lines for the detection of ABA-activated protein kinases. Proteins were electrophoresed on an SDS-polyacrylamide gel containing histone H1S. After denaturation and renaturation procedures, the proteins were reacted with γ -[32 P]ATP. (Lower) Coomassie Brilliant Blue (CBB) staining of ribulose 1,5-bisphosphate carboxylase/oxygenase. (B) The ARK-GFP construct fused to the CaMV35 promoter was introduced into protonema cells of *P. patens*. Localization of GFP and PpSnRK2B-GFP is shown for comparison. (C) Kinase activity of GST-ARK^{KD} on MBP-PpSnRK2B. Recombinant proteins of MBP-PpSnRK2B (1 μ g) (lanes 1 and 3) and GST-ARK^{KD} (0.05 μ g) (lanes 2 and 3) were reacted with γ -[32 P]ATP and electrophoresed on an SDS-polyacrylamide gel, followed by Coomassie Brilliant Blue staining and autoradiography (32 P). Closed and open arrowheads indicate the positions of MBP-PpSnRK2B and GST-ARK^{KD}, respectively. (D) In-gel kinase assays of the recombinant MBP-PpSnRK2B (1 μ g) with or without autophosphorylation (Auto-P) or phosphorylation by GST-ARK^{KD} (0.05 μ g). Positions of molecular-weight markers are shown in kilodaltons. Results of staining with Coomassie Brilliant Blue and immunoblot analysis using the anti-ARK antibody (Anti-ARK) are shown for comparison. Closed and open arrowheads indicate the positions of MBP-PpSnRK2B and GST-ARK^{KD}, respectively. (E) Phosphorylation sites in the activation loop of MBP-PpSnRK2B identified by phosphopeptide mapping. The amino acid sequence and probable phosphorylation sites (asterisks) of the identified phosphopeptide ($m/z = 924.46$) and its ion-current chromatograms are shown. The MBP-PpSnRK2B protein was either phosphorylated with GST-ARK^{KD} or autophosphorylated (Auto-P) for 15 min. (Details are shown in Fig. S6.)

and VIII in the activation loop, has been identified as the critical Ser residue for the activation of *Arabidopsis* SnRK2s (27).

To explore possible regulation of ARK, we also examined the phosphorylation status of ARK. Proteins extracted from transgenic *P. patens* expressing ARK-GFP (Fig. 3B) were subjected to purification by magnetic beads with the anti-GFP antibody attached, and the purified proteins were used for phosphopeptide mapping. We identified phosphorylation of a peptide corresponding to amino acids 1029–1043 of ARK, with phosphorylation on either Ser-1029 or Ser-1030 (Fig. 4A). These residues were located within the activation loop in the kinase domain, comparable with phosphorylation sites of other eukaryotic MAPKKs (Fig. 4B). To determine the role of phosphorylation of ARK, mutation constructs were generated by replacing both Ser-1029 and Ser-1030, or either, with Ala, and the constructs were used for transient assays in AR7 cells with *Em-GUS* to determine their capacity to restore ABA responsiveness (Fig. 4C). We found that ARK with Ala substitution of Ser-1029 (S1029A) does not restore ABA-induced *Em-GUS* expression in AR7. When both Ser-1029 and Ser-1030 were replaced with Ala (S1029A/S1030A), the *GUS* expression level was as low as in the Ser-1029 mutation, whereas replacing only Ser-1030 with Ala (S1030A) restored *Em-GUS*

expression to a level similar to that in nonmutated ARK. These results indicate that phosphorylation of ARK at Ser-1029 in the activation loop is essential for its activation.

Functional Complementation of the *Ark* Mutation by B3-MAPKKs from Other Land Plant Sources. To determine the diversity of ARK-related genes in land plants, phylogenetic analysis of group B1–B4 Raf-like MAPKKs from *P. patens*, *A. thaliana*, and *Selaginella moellendorffii* (Fig. 5A) was conducted. Three and six members of B3-MAPKKs are encoded in the genomes of *S. moellendorffii* and *A. thaliana*, respectively, whereas ARK is the only B3-MAPKK in *P. patens*. Furthermore, the *S. moellendorffii* and *A. thaliana* genomes encode two and six B2-MAPKKs, respectively, but they were not found in the *P. patens* genome. The genes for group B1 MAPKK (B1-MAPKK) appeared to be the closest relatives of ARK in *P. patens*. To determine the functional relevance of the B1-MAPKK genes to ARK, we examined whether the introduction of these B1-MAPKK genes can restore ABA-induced *GUS* expression of AR7 by a transient assay. Introduction of two B1-MAPKKs (*PpIs63_65V6.1* and *PpIs75_1V6.1*) did not restore ABA-induced *Em-GUS* expression in AR7, indicating that the response is specific to ARK belonging to group B3 (Fig. 5B).

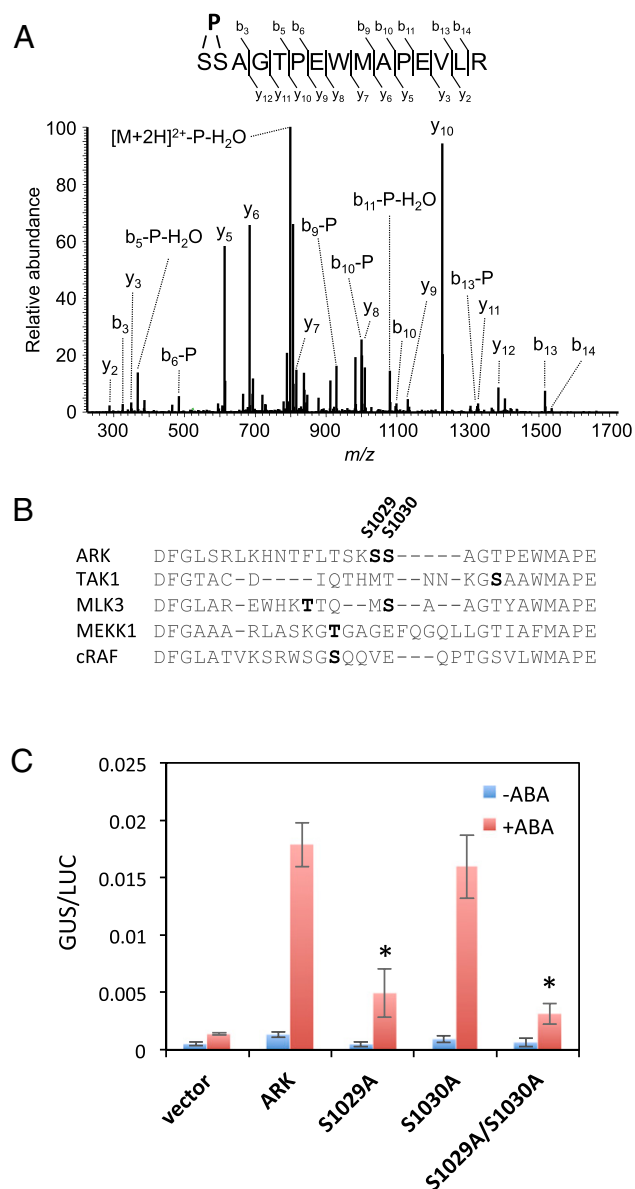


Fig. 4. Phosphorylation in the activation loop of ARK is essential for ABA response. (A) MS/MS spectrum of the ARK-derived phosphopeptide found to be increased by ABA treatment in protonemata. Proteins were purified from ABA-treated protonemata of *P. patens* expressing ARK-GFP by using magnetic beads with the anti-GFP antibody attached. The purified proteins were subjected to digestion with Lys-C and trypsin and analysis by a nanoLC-MS-MS system. Either Ser-1029 or Ser-1030 was predicted to be the site of phosphorylation. (B) Sequence alignment of the amino acids in the activation loop of ARK and mammalian MAPKKs. Predicted phosphorylation sites for ARK (S1029 and S1030), TAK1 (46), MLK3 (47), MEKK1 (48), and cRAF (49) are indicated by bold letters. (C) Transient assays of AR7 protonemata using constructs of ARK-GFP with or without mutations in the predicted phosphorylation sites. The cDNA was fused to the rice actin promoter and introduced into the AR7 cells with *Em-GUS* and *Ubi-LUC*, and the cells were incubated for 1 d with or without 10 μ M ABA before protein extraction for the GUS and LUC assays. Levels of gene expression are represented by GUS/LUC ratio. Error bars indicate the SE ($n = 3$). * $P < 0.05$ compared with the ARK-GFP-introduced cells (t -test).

We further tested whether B3-MAPKKK genes from *A. thaliana* and *S. moellendorffii* can complement ABA insensitivity of AR7 by transient assays. Fig. 5C shows that *A. thaliana* cDNA clones for *Atlg73660* and *At4g24480* and the *S. moellendorffii* cDNA clone for *Sm269874* restored ABA-induced *Em-GUS* expression in AR7.

Results of experiments using other B3-MAPKKK clones indicated that *Atlg18160* also restored the GUS expression in AR7, but *At5g11850*, *At5g03730*, and *Atlg08720* had little effect (Fig. S7). These results indicated that specific genes of vascular plants encoding B3-MAPKKK can functionally complement the impairment of ARK in the moss.

Discussion

Although subclass III SnRK2 is recognized as a key regulator of ABA signaling, the mode of kinase activity regulation has not been fully elucidated. A generally accepted mechanism of SnRK2 activation is that ABA suppresses PP2C activity via binding to PYR/PYL/RCAR receptors, thus facilitating enhancement of autophosphorylation of SnRK2 (11). In *Arabidopsis*, activity of SnRK2.2, SnRK2.3, and SnRK2.6 was increased in the triple mutant of group A PP2C (*abilhab1pp2ca*), indicating that inhibition of the PP2C by the ABA-receptor complex is the key mechanism for activation of SnRK2 by autophosphorylation (28). The present study of ARK, a group B3 Raf-like kinase, provides evidence of positive regulation of ABA signaling in addition to negative regulation by group A PP2Cs in bryophytes. Plant Raf-like kinases have been shown to function in various types of biotic and abiotic signaling, but they are not thought to function in a typical MAP kinase pathway involving MAP kinase kinases and MAP kinases, and there is little biochemical evidence regarding their target substrates (29). This result is consistent with our observation of little ABA-induced kinase activity when myelin basic protein, a substrate commonly used for detection of MAP kinases, was used for in-gel kinase assays. Our study showing that a specific Raf-like kinase functions for activation of SnRK2 provides new insights into a signaling pathway for a possible connection between these kinases through unidentified mechanisms operating in plant ABA response.

Our study also indicated the possible mechanism for hyperosmosis-induced activation of plant SnRK2s mediated by an upstream protein kinase. SnRK2s representing all three subclasses in *Arabidopsis* and rice are activated by hyperosmosis (8, 10), but the mechanism of activation has not been elucidated. Results of a previous report indicated that hyperosmosis-induced SnRK2 activation might involve unidentified upstream protein kinases that phosphorylate SnRK2s (27). The reduced hyperosmosis-induced kinase activity in AR7 indicated that ARK might be involved in the activation of SnRK2 (Fig. 1C) toward osmostress tolerance (Fig. 2E). Hyperosmosis response by both ABA-dependent and independent mechanisms in the moss has been demonstrated recently using an ABA-deficient mutant of *P. patens* (30). Given that both mechanisms are mediated by ARK, this kinase is possibly a regulatory target of ABA and hyperosmotic signals upstream of SnRK2s.

Phosphopeptide mapping and mutational analysis of transient assays indicated that ARK itself might be activated by phosphorylation in the activation loop (Fig. 4A and C). Activation by phosphorylation in the activation loop is well defined in mammalian and yeast MAPKKs (Fig. 4B). Phosphorylation and activation events in these kinases typically are modulated through their nonkinase domain by dimerization, binding of other regulatory proteins, or phosphorylation by upstream MAPKKK kinases (31). The loss of ARK function with the Ser-to-Phe substitution at position 532 in the nonkinase domain (Fig. 2A–G) suggests that the region around Ser-532 functions as a regulatory domain, and the Ser-to-Phe alteration might have resulted in a drastic change in microenvironment of the region because of the introduction of a bulky hydrophobic residue, leading to the abolishment of the kinase activity by an unidentified mechanism. The role of the N-terminal nonkinase domain in the regulation of kinase activity is well defined in Ste11p MAPKKK in budding yeast (32), wherein an intramolecular autoinhibitor sequence in the N-terminal domain interacts with the C-terminal kinase domain to inhibit its catalytic activity. The inhibition is enhanced by the binding of Ste50p to the N-terminal domain and is ameliorated

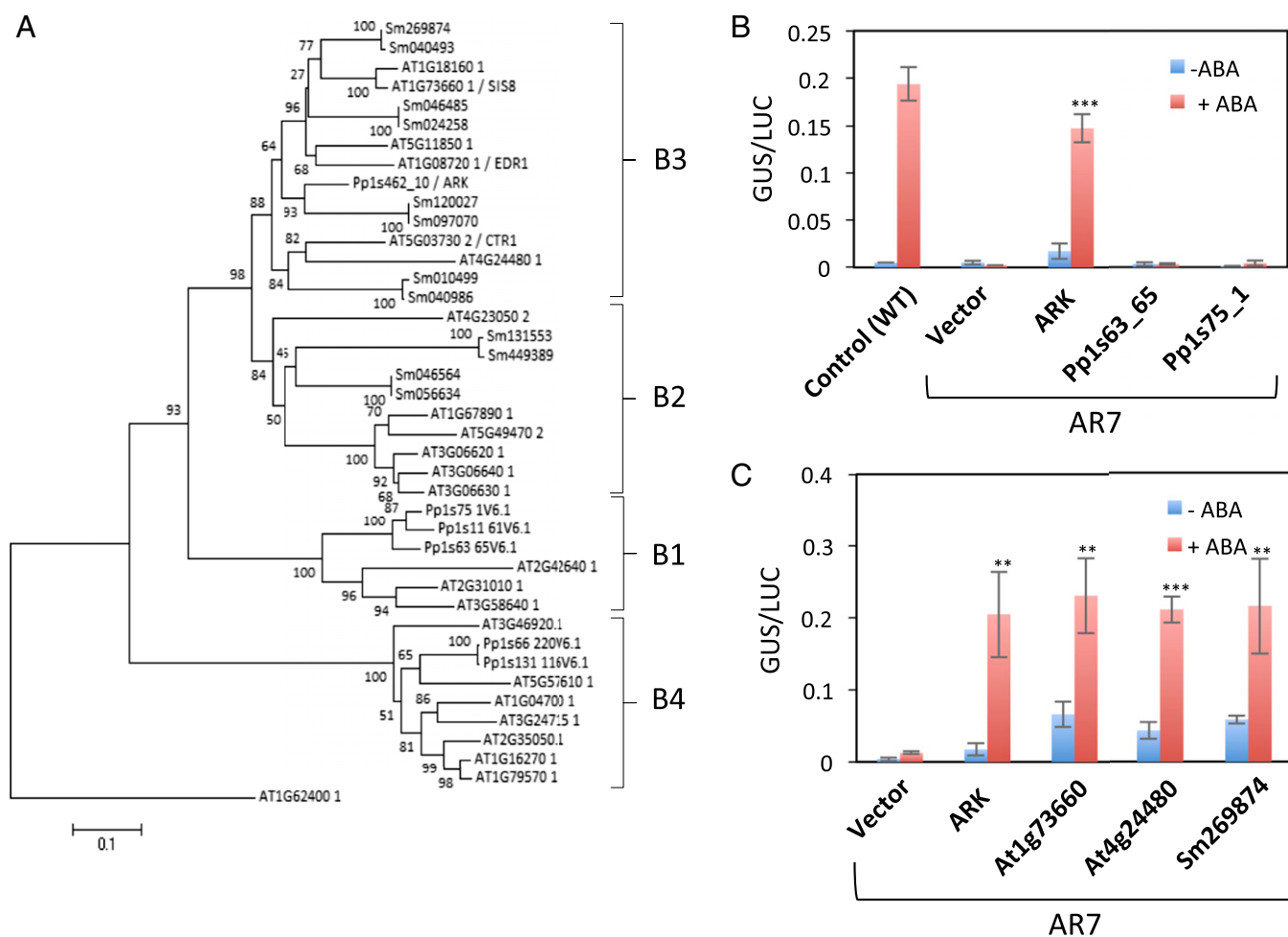


Fig. 5. Phylogenetic and functional analyses of group B3 Raf-like MAPKKs in land plants. (A) Phylogenetic analysis of plant Raf-like MAPKKs belonging to groups B1–B4 in *P. patens*, *S. moellendorffii*, and *A. thaliana*. (B and C) Transient assays of *P. patens* protonemata using various MAPKK DNA clones. The cDNA clones were fused to the rice actin promoter and were cointroduced with *Em-GUS* and *Ubi-LUC* into protonemata. The protonemata were incubated with or without ABA for 1 d and were used for GUS and LUC assays. Error bars indicate the SE ($n = 3$). *** $P < 0.001$ and ** $P < 0.01$ compared with the vector control (t-test). (B) Results for ARK and two group B1 MAPKKs, *Pp1s63_65V6.1* and *Pp1s75_1V6.1*. (C) Results for ARK, two *Arabidopsis* genes, *At1g73660* and *At4g24480*, and one Selaginella gene, *Sm269874*.

upon signal perception by phosphorylation at the specific Ser and Thr residues by an upstream kinase Ste20p. The role of the N-terminal domain in stimulating ARK phosphorylation and how ABA facilitates this process have not been clarified.

ARK is the sole B3-MAPKKK in *P. patens*, but angiosperms have multiple B3-MAPKKKs with various functions. *CONSTITUTIVE TRIPLE RESPONSE1* (*CTR1*, *At5g03730*) is well known as a negative regulator of ethylene signaling (33). *ENHANCED DISEASE RESISTANCE1* (*EDR1*, *At1g08720*) and *At1g73660* have been demonstrated to be involved in salicylic acid-induced defense responses (34) and in salt tolerance (35), respectively. Evidence of signal crosstalk between these apparently unrelated stimuli has been provided by analysis of *Arabidopsis* mutants. For instance, the *ctr1* mutant allele has been isolated as a mutant that enhances ABA insensitivity of *abi1-1* (36). The *ctr1* allele also has been identified as a mutant defective in sugar response (37, 38). From studies using various other mutants, signal crosstalk among ABA, sugar, and ethylene in *Arabidopsis* has been proposed (39), although details of the mechanism have not been clarified. *At1g73660*, identified as the *at6* locus that improves salt-stress tolerance (35), also has been identified as the gene responsible for *sugar insensitive8* (*sis8*) showing sugar-resistant seedling growth (40, 41). The loss-of-function mutant of *At1g73660*, however, exhibited a WT response

to ABA, the gibberellic acid biosynthesis inhibitor paclobutrazol, and the ethylene precursor aminocyclopropane carboxylic acid in germination experiments (35, 40), indicating that *At1g73660* has a distinct function specific to salt and sugar. We hypothesize that the prototype B3-MAPKKK (ARK), mainly engaged in ABA and hyperosmotic responses in ancestral land plants, had diversified in vascular plants by acquiring more specialized functions toward sugar, salt, ethylene, and pathogenic signals. It should be noted that restoration of ABA-induced gene expression in AR7 by some of *Arabidopsis* B3-MAPKKKs (Fig. 5C) does not necessarily reflect physiological events during the ABA response in angiosperms. Whether any of the B3-MAPKKKs in angiosperms are involved in the positive regulation of SnRK2 would be clarified by detailed analysis of the mutants of B3-MAPKKKs with respect to ABA response and SnRK2 activation.

Experimental Procedures

Plant Materials, Growth Conditions, and Acclimation Treatment. Protonema tissues of *P. patens* (Hedw.) Bruch & Schimp. were grown on cellophane-overlaid 0.8% agar plates of BCDAT medium supplemented with 0.5% glucose (42). The protonemata were cultured in a controlled environment growth chamber at 25 °C under continuous illumination (35 $\mu\text{mol photons}\cdot\text{m}^{-2}\cdot\text{s}^{-1}$). ABA, cold, and hyperosmotic treatments of the protonemata were carried out as described previously (22, 30).

Transcriptome Analysis. Microarray analysis was carried out using a *P. patens* custom oligonucleotide microarray in which 33,942 gene-specific probes were mounted in an Agilent format microarray as described previously (20). Protonemata of the WT line and AR7 cultured on normal BCDAT medium or medium containing 10 μ M ABA for 6 h were used for RNA extraction. One microgram of total RNA for each sample was used for RNA synthesis using the Amino Allyl MessageAmp II aRNA Amplification Kit (Life Technologies). The aRNA were labeled with Cy5 and Cy3 using the same kit. Fluorescent probes were hybridized on the array at 65 °C for 16 h by a dye-swap experimental procedure. The microarray was scanned with a GenePix 4000B system (Molecular Devices). Digitalization of signal intensities and calculation of the Cy5/Cy3 ratio were performed with Genepix Pro-6.0 software (Molecular Devices). In this process, quality control was carried out with signal values; probes with saturated intensity values (65,535) or a low signal-to-noise ratio (<3) were removed. Normalization was done by the Lowess (Locally Weighted Scatter plot Smoother) method. After filtering for intensity value, a total of 14,034 probes were subjected to further analysis. Fold-change analysis was performed on double replicate samples to determine the genes decreased in AR7. A twofold expression cutoff was considered to determine the genes decreased in AR7. ABA-regulated genes used for the analysis were described previously (20). The microarray data were deposited in Gene Expression Omnibus (accession GSE68914).

Transformation of *P. patens*. A gene knock-in construct was made by amplification of the DNA fragment of genomic regions of *ARK* and fusion with the resistant cassette *CaMV35S::NptII::NOS* of pTN82 (a generous gift from Mitsuyasu Hasebe, National Institute for Basic Biology, Okazaki, Japan). Transformation of *P. patens* was carried out by the polyethylene glycol-mediated method as described previously (42).

Total RNA Preparation and RNA Gel Blot Analysis. RNA extraction, electrophoresis, and blotting onto a nylon membrane were carried out according to the method described previously (22). The RNAs blotted on the membrane were hybridized with radiolabeled probes of *17B9* (*Pp1s294_52V6.1*), *LEAIII* (*Pp1s118_232V6.1*), *Blt* (*Pp1s2_779V6.1*), *LEA172* (*Pp1s370_29V6.1*), and *6A5* (*Pp1s267_21V6.1*) (22, 30, 43). Hybridization was carried out using Ultrahyb hybridization buffer (Ambion) at 42 °C overnight. Posthybridization washings were carried out at 65 °C for 1 h in a buffer containing 0.2 \times SSC (1 \times SSC containing 150 mM NaCl and 15 mM Na citrate) and 0.2% SDS. Hybridizing signals were detected by exposure to X-ray film.

Comparative Genomic Analysis. Sequencing libraries were prepared using the NEBNext DNA Sample Prep Reagent Set 1 (New England Biolabs) following the manufacturer's protocols. Briefly, 3 μ g of genomic DNA was fragmented to an average length of 300 bp by the Covaris S2 system (Covaris). After repair of the fragmented DNA, a single A nucleotide was ligated to the 3' end. Illumina Index PE adaptors (Illumina) were ligated to the fragments, and fragments between 350 and 450 bp were selected with a 1.5% Pippin prep gel (Sage Science). The size-selected product was amplified by PCR for 12 cycles with primers InPE1.0, InPE2.0, and Index primer containing a unique index tag for each individual sample. The final product was validated by Agilent Bioanalyzer 2100 (Agilent). Pooled libraries were sequenced on HiSeq 2000 (Illumina) following the manufacturer's protocol, generating 100-bp paired-end reads and 6-bp index tags. All FASTQ files were imported to CLC Genomics Workbench software ver. 5.5.1 (CLC bio). After the quality of each FASTQ file had been evaluated, reads were mapped to the reference genome of *P. patens* (downloaded from genome.jgi.doe.gov/PhytozomeV9/download/_JAMO/52b9c81b166e730e43a34f83/Ppatens_152.fa.gz) using default parameters. Variants were detected using the probabilistic variant detection function with following parameters: minimum coverage = 5, maximum expected variants = 1, ignore quality scores = no, ignore non-specific matches = yes, ignore broken pairs = no, filter 454/Ion homopolymer indels = no, variant probability = 90.0, require presence in both forward and reverse reads = yes. Nonsynonymous substitutions were detected using the "Amino Acid Changes" tool of CLC Genomics Workbench with reference to the *P. patens* ver.1.6 coding sequences.

Transient Assays of *P. patens* Protonemata. Protonemata of *P. patens* cultured on the BCDAT agar medium were bombarded with *Em-GUS* and *Ubi-LUC* by using the PDS-1000He particle delivery system (Bio-Rad) with 1- μ m gold particles and 1,100-psi rupture discs under a vacuum of 26 mmHg. The bombarded protonemata were cultured at 25 °C under continuous light for 24 h on BCDAT agar medium with or without 10 μ M ABA. Proteins extracted from the protonemata were used for GUS and LUC assays to determine the GUS/LUC ratio as previously described (44).

Tests for Freezing Tolerance and Hyperosmotic-Stress Tolerance. The freezing tolerance of *P. patens* protonemata was determined as described previously (30). In brief, protonema tissues placed in a glass test tube were seeded with ice at -1 °C, kept at -1 °C for 50 min, and then cooled at a rate of -2.4 °C/h to desired temperatures. Electrolyte leakage from the damaged tissues was measured after thawing by using a conductivity meter and was represented as the percentage of total ions released after subsequent boiling (1). For osmotic stress treatment, the tissues were placed on a medium containing 0.4 M mannitol and were grown for 7 d under continuous light.

Analysis Using GFP-Fusion Constructs. GFP-fusion constructs of *ARK* and *PpSnRK2B* were generated by fusing the cDNA to *CaMV35S::SGFP(S65T)* (45) using the *NcoI* site at start codon of GFP. Five-day-old *P. patens* protonemata were bombarded with the GFP-fusion constructs, and cells were observed under a confocal laser-scanning microscope.

Preparation of Recombinant Proteins. For preparation of MBP-PpSnRKB, the entire coding sequence of *PpSnRKB* cDNA (*Pp1s240_91V6.1*) was amplified from reverse transcripts of *P. patens* protonemata and fused in-frame to the *NdeI*-digested pMAL-c5X vector (New England Biolabs). The MBP-fusion protein was purified using amylose resin according to the manufacturer's instructions. For GST-ARK^{KD}, the region of the protein kinase domain (amino acids 867–1148) was fused in-frame to the *BamHI*/*NotI*-digested pGEX-5 \times 3 vector (GE Healthcare). The GST-fusion protein was purified using glutathione-Sepharose resin. Both recombinant proteins were subjected to ultrafiltration using a Nanosep 30-kDa size-exclusion column (Pall) for concentration and removal of low-molecular-weight materials.

Immunoblot Analysis. Proteins electrophoresed on 10% (wt/vol) SDS-polyacrylamide gels were transferred onto PVDF membranes, reacted with primary and secondary antibodies, and detected by either nitroblue tetrazolium/5-bromo-4-chloro-3-indolyl phosphate reagent or chemiluminescent reagents. For preparation of ARK antibodies, antiserum raised against the C-terminal 15 amino acids (LGSTPKSGLSDRDL) of ARK was subjected to affinity purification using the recombinant GST-ARK^{KD} protein fixed on a PVDF membrane.

Protein Kinase Assays. In vitro phosphorylation reactions were carried out using affinity-purified recombinant proteins at 30 °C for 15 min in 50 mM Tris-Cl (pH 7.5), 10 mM MgCl₂, 1 mM DTT, and 50 μ M γ -[³²P]ATP. The reaction mixture was electrophoresed on an SDS-polyacrylamide gel and stained with Coomassie Brilliant Blue, and phosphoproteins were detected by autoradiography. In-gel kinase assays were carried out essentially as described previously (20). In brief, 50 μ g of total soluble proteins extracted from ABA-treated and nontreated protonemata were electrophoresed using SDS-polyacrylamide gel containing histone III_S (H5055; Sigma). After denaturation and renaturation procedures, the gel was incubated with 50 μ M γ -[³²P]ATP. The gel was washed, dried, and exposed to X-ray film to detect kinase activity. For recombinant proteins, the kinase reaction was carried out at 30 °C for 15 min in 50 mM Tris-Cl (pH 7.5), 10 mM MgCl₂, and 1 mM DTT with 50 μ M nonradioactive ATP, and the reaction mixture was loaded onto the histone III_S-polymerized polyacrylamide gel for in-gel kinase assays.

Phosphopeptide Mapping. Protonemata of *P. patens* expressing ARK-GFP were used for protein extraction. The ARK-GFP proteins were purified by using anti-GFP magnetic microbeads (Miltenyi Biotec) according to the manufacturer's instructions. Determination of phosphorylation sites of proteins was carried out essentially as described previously (12). Phosphorylated proteins digested with Lys-C and trypsin were analyzed by a nanoLC-MS/MS system for peptide identification, quantification, and prediction of phosphorylation sites. For enrichment of phosphopeptides, the digested peptides were subjected to hydroxyl acid-associated metal oxide affinity chromatography.

ACKNOWLEDGMENTS. We thank Ralph Quatrano for *Em-GUS*, Tuan-hua David Ho for *Ubi-LUC*, Yasuo Niwa for 35S-sGFP(S65T), Mitsuyasu Hasebe for pTN82, and the NODAI Genome Research Center of Tokyo University of Agriculture for the use of Illumina HiSeq 2000. This study was supported in part by Grants-in-Aid for Scientific Research 26291054, 23119504, and 25119705 from the Ministry of Education, Culture, Sports, Science, and Technology of Japan (to D.T.), 24570058 and 16780235 (to Y. Sakata), and 25840103 and 15H04383 (to T.U.); by Grant for Basic Science Research Projects 110493 from The Sumitomo Foundation (to Y. Sakata); and by Precursory Research for Embryonic Science and Technology (PRESTO) from Japan Science and Technology Agency (T.U.).

1. Nagao M, Minami A, Arakawa K, Fujikawa S, Takezawa D (2005) Rapid degradation of starch in chloroplasts and concomitant accumulation of soluble sugars associated with ABA-induced freezing tolerance in the moss *Physcomitrella patens*. *J Plant Physiol* 162(2):169–180.
2. Cuming AC, Cho SH, Kamisugi Y, Graham H, Quatrano RS (2007) Microarray analysis of transcriptional responses to abscisic acid and osmotic, salt, and drought stress in the moss, *Physcomitrella patens*. *New Phytol* 176(2):275–287.
3. Khandelwal A, et al. (2010) Role of ABA and ABI3 in desiccation tolerance. *Science* 327(5965):546.
4. Li J, Wang XQ, Watson MB, Assmann SM (2000) Regulation of abscisic acid-induced stomatal closure and anion channels by guard cell AAPK kinase. *Science* 287(5451):300–303.
5. Assmann SM (2003) *OPEN STOMATA1* opens the door to ABA signaling in *Arabidopsis* guard cells. *Trends Plant Sci* 8(4):151–153.
6. Umezawa T, et al. (2010) Molecular basis of the core regulatory network in ABA responses: Sensing, signaling and transport. *Plant Cell Physiol* 51(11):1821–1839.
7. Fujita Y, Yoshida T, Yamaguchi-Shinozaki K (2013) Pivotal role of the AREB/ABF-SnRK2 pathway in ABRE-mediated transcription in response to osmotic stress in plants. *Physiol Plant* 147(1):15–27.
8. Kobayashi Y, Yamamoto S, Minami H, Kagaya Y, Hattori T (2004) Differential activation of the rice sucrose nonfermenting1-related protein kinase2 family by hyperosmotic stress and abscisic acid. *Plant Cell* 16(5):1163–1177.
9. Umezawa T, Yoshida R, Maruyama K, Yamaguchi-Shinozaki K, Shinozaki K (2004) SRK2C, a SNF1-related protein kinase 2, improves drought tolerance by controlling stress-responsive gene expression in *Arabidopsis thaliana*. *Proc Natl Acad Sci USA* 101(49):17306–17311.
10. Boudsocq M, Barbier-Brygoo H, Laurière C (2004) Identification of nine sucrose nonfermenting 1-related protein kinases 2 activated by hyperosmotic and saline stresses in *Arabidopsis thaliana*. *J Biol Chem* 279(40):41758–41766.
11. Fujii H, et al. (2009) In vitro reconstitution of an abscisic acid signalling pathway. *Nature* 462(7273):660–664.
12. Umezawa T, et al. (2009) Type 2C protein phosphatases directly regulate abscisic acid-activated protein kinases in *Arabidopsis*. *Proc Natl Acad Sci USA* 106(41):17588–17593.
13. Yoshida R, et al. (2006) The regulatory domain of SRK2E/OST1/SnRK2.6 interacts with ABI1 and integrates abscisic acid (ABA) and osmotic stress signals controlling stomatal closure in *Arabidopsis*. *J Biol Chem* 281(8):5310–5318.
14. Ma Y, et al. (2009) Regulators of PP2C phosphatase activity function as abscisic acid sensors. *Science* 324(5930):1064–1068.
15. Park S-Y, et al. (2009) Absciscic acid inhibits type 2C protein phosphatases via the PYR/PYL family of START proteins. *Science* 324(5930):1068–1071.
16. Soon F-F, et al. (2012) Molecular mimicry regulates ABA signaling by SnRK2 kinases and PP2C phosphatases. *Science* 335(6064):85–88.
17. Rensing SA, et al. (2008) The *Physcomitrella* genome reveals evolutionary insights into the conquest of land by plants. *Science* 319(5859):64–69.
18. Sakata Y, Komatsu K, Takezawa D (2014) ABA as a universal plant hormone. *Prog Bot* 75:57–96.
19. Chater C, et al. (2011) Regulatory mechanism controlling stomatal behavior conserved across 400 million years of land plant evolution. *Curr Biol* 21(12):1025–1029.
20. Komatsu K, et al. (2013) Group A PP2Cs evolved in land plants as key regulators of intrinsic desiccation tolerance. *Nat Commun* 4:2219.
21. Minami A, Togawa S, Nagao M, Takezawa D (2006) Altered freezing tolerance in the *Physcomitrella patens* mutant with reduced sensitivity to abscisic acid. *Cryobiol Cryotechnol* 52(2):135–139.
22. Bhyan SB, et al. (2012) Cold acclimation in the moss *Physcomitrella patens* involves abscisic acid-dependent signaling. *J Plant Physiol* 169(2):137–145.
23. Marcotte WR, Jr, Russell SH, Quatrano RS (1989) Absciscic acid-responsive sequences from the em gene of wheat. *Plant Cell* 1(10):969–976.
24. Knight CD, et al. (1995) Molecular responses to abscisic acid and stress are conserved between moss and cereals. *Plant Cell* 7(5):499–506.
25. Hefti MH, François K-J, de Vries SC, Dixon R, Vervoort J (2004) The PAS fold. A re-definition of the PAS domain based upon structural prediction. *Eur J Biochem* 271(6):1198–1208.
26. Ichimura K, et al.; MAPK Group (2002) Mitogen-activated protein kinase cascades in plants: A new nomenclature. *Trends Plant Sci* 7(7):301–308.
27. Boudsocq M, Droillard MJ, Barbier-Brygoo H, Laurière C (2007) Different phosphorylation mechanisms are involved in the activation of sucrose non-fermenting 1 related protein kinases 2 by osmotic stresses and abscisic acid. *Plant Mol Biol* 63(4):491–503.
28. Ng LM, et al. (2011) Structural basis for basal activity and autoactivation of abscisic acid (ABA) signaling SnRK2 kinases. *Proc Natl Acad Sci USA* 108(52):21259–21264.
29. Menges M, et al. (2008) Comprehensive gene expression atlas for the *Arabidopsis* MAP kinase signalling pathways. *New Phytol* 179(3):643–662.
30. Takezawa D, et al. (2015) Epoxycarotenoid-mediated synthesis of abscisic acid in *Physcomitrella patens* implicating conserved mechanisms for acclimation to hyperosmosis in embryophytes. *New Phytol* 206(1):209–219.
31. Kolch W (2000) Meaningful relationships: The regulation of the Ras/Raf/MEK/ERK pathway by protein interactions. *Biochem J* 351(Pt 2):289–305.
32. Drogen F, et al. (2000) Phosphorylation of the MEKK Ste11p by the PAK-like kinase Ste20p is required for MAP kinase signaling in vivo. *Curr Biol* 10(11):630–639.
33. Kieber JJ, Rothenberg M, Roman G, Feldmann KA, Ecker JR (1993) CTR1, a negative regulator of the ethylene response pathway in *Arabidopsis*, encodes a member of the raf family of protein kinases. *Cell* 72(3):427–441.
34. Frye CA, Innes RW (1998) An *Arabidopsis* mutant with enhanced resistance to powdery mildew. *Plant Cell* 10(6):947–956.
35. Gao L, Xiang CB (2008) The genetic locus At1g73660 encodes a putative MAPKKK and negatively regulates salt tolerance in *Arabidopsis*. *Plant Mol Biol* 67(1–2):125–134.
36. Beaudoin N, Serizet C, Gosti F, Giraudat J (2000) Interactions between abscisic acid and ethylene signaling cascades. *Plant Cell* 12(7):1103–1115.
37. Zhou L, Jang JC, Jones TL, Sheen J (1998) Glucose and ethylene signal transduction crosstalk revealed by an *Arabidopsis* glucose-insensitive mutant. *Proc Natl Acad Sci USA* 95(17):10294–10299.
38. Gibson SI, Laby RJ, Kim D (2001) The sugar-insensitive1 (sis1) mutant of *Arabidopsis* is allelic to ctr1. *Biochem Biophys Res Commun* 280(1):196–203.
39. Rolland F, Baena-Gonzalez E, Sheen J (2006) Sugar sensing and signaling in plants: Conserved and novel mechanisms. *Annu Rev Plant Biol* 57:675–709.
40. Laby RJ, Kincaid MS, Kim D, Gibson SI (2000) The *Arabidopsis* sugar-insensitive mutants sis4 and sis5 are defective in abscisic acid synthesis and response. *Plant J* 23(5):587–596.
41. Huang Y, Li CY, Qi Y, Park S, Gibson SI (2014) SIS8, a putative mitogen-activated protein kinase kinase kinase, regulates sugar-resistant seedling development in *Arabidopsis*. *Plant J* 77(4):577–588.
42. Nishiyama T, Hiwatashi Y, Sakakibara I, Kato M, Hasebe M (2000) Tagged mutagenesis and gene-trap in the moss, *Physcomitrella patens* by shuttle mutagenesis. *DNA Res* 7(1):9–17.
43. Minami A, Nagao M, Arakawa K, Fujikawa S, Takezawa D (2006) Physiological and morphological alteration associated with freezing tolerance in the moss *Physcomitrella patens*. *Cold Hardiness in Plants: Molecular Genetics, Cell Biology and Physiology*, eds Chen T, Uemura M (CABI, Wallingford), pp 138–152.
44. Komatsu K, et al. (2009) Functional analyses of the ABI1-related protein phosphatase type 2C reveal evolutionarily conserved regulation of abscisic acid signaling between *Arabidopsis* and the moss *Physcomitrella patens*. *Plant Mol Biol* 70(3):327–340.
45. Niwa Y (2003) A synthetic green fluorescent protein gene for plant biotechnology. *Plant Biotechnol* 20(1):1–11.
46. Kishimoto K, Matsumoto K, Ninomiya-Tsuji J (2000) TAK1 mitogen-activated protein kinase kinase kinase is activated by autophosphorylation within its activation loop. *J Biol Chem* 275(10):7359–7364.
47. Leung IW, Lassam N (2001) The kinase activation loop is the key to mixed lineage kinase-3 activation via both autophosphorylation and hematopoietic progenitor kinase 1 phosphorylation. *J Biol Chem* 276(3):1961–1967.
48. Deak JC, Templeton DJ (1997) Regulation of the activity of MEK kinase 1 (MEKK1) by autophosphorylation within the kinase activation domain. *Biochem J* 322(Pt 1):185–192.
49. Kolch W, et al. (1993) Protein kinase C α activates RAF-1 by direct phosphorylation. *Nature* 364(6434):249–252.